POLARIZATION OBSERVABLES IN THE N→Δ(1232) TRANSITION

SALVATORE FRULLANI
INFN,Gruppo Sanità and Istituto Superiore di Sanità,Physics Laboratory - Rome, Italy

JAMES J. KELLY
University of Maryland, Department of Physics - College Park, MD 20742, U.S.A.

ADAM J. SARTY
Saint Mary's University,Department of Astronomy & Physics - Halifax, NS, Canada

ROBERT W. LOURIE
Renaissance Technologies Corporation, East Setauket, NY 11733-2841, U.S.A.

MARK K. JONES AND DAVE G. MEEKINS
Thomas Jefferson National Accelerator Facility, Newport News, VA 23606, U.S.A.

WILLIAM BERTOZZI, ZHENGWEI CHAI AND SHALEV GILAD
M.I.T., Department of Physics - Cambridge, MA 02139, U.S.A.

RIKKI E. ROCHÉ
Florida State University, Physics Department - Tallahassee, FL 32306, U.S.A.

AND

THE JEFFERSON LAB HALL A COLLABORATION

1. Introduction

In the simple SU(6) spherically symmetric quark model, the proton and the $\Delta(1232)$ are states of three quarks in an overall S-wave with spins coupled to 1/2 and 3/2 respectively. In this context, the transition has a pure magnetic dipole M_{1+} nature resulting in the spin-flip of a single quark. However the measurements carried out in the late sixties and early seventies at DESY [1, 2, 3], NINA (Daresbury) [4] and CEA (Harvard) [5] have demonstrated already the inconsistency of the data with a pure magnetic dipole transition, indicating that, although small, other components were also needed.

Due to selection rules, the only other resonant multipole contributions to the excitation of the $\Delta(1232)$ are the Coulomb quadrupole S_{1+} and the electric quadrupole E_{1+}. These quadrupolar transitions imply non-spherical forces - whose dynamical origin is ascribed to different mechanisms by the various models (see as examples [6, 7, 8]) - which could result in a L=2 component in the nucleon or/and delta wave functions. This problem is obviously of interest for the spin physics studied in polarized deep inelastic scattering in connection with the question of the contribution of quarks and gluons orbital angular momenta to the nucleon spin.

In addition to the resonant transitions other coherent nonresonant processes and tails of transitions to higher energy resonances contribute as background to the yield under the Δ peak . These processes must be determined or at least constrained with measurements and model computations in order to extract in a reliable way the strength of the S_{1+} and E_{1+} contributions to the N$\rightarrow\Delta(1232)$ transition.

Due to the smallness of other components with respect to the magnetic dipole transition the most useful way to quantify their importance is through the simultaneous measurement of observables that depend linearly on interference terms of one of the small components with the dominant (M_{1+}).

The previously mentioned old experimental data, resulting from measurements carried out with unpolarized, low duty cycle and low intensity beams, allowed the determination of a small number of observables with large uncertainties and with the consequent unsatisfactory knowledge about the quadrupolar components. The new facilities like MAMI, ELSA, LEGS, Bates-MIT and Jlab have renewed, in recent years, the interest on the subject motivating measurements of high quality.

In figure 1 most of the available data on the extracted Coulomb and electric quadrupole terms are shown. The situation is sensibly improved with new results in very recent years both in photo and electro-production. However, due to the complexity of data reduction, results obtained from measurements using different techniques have to be compared in order to fully size systematic and model dependent uncertainties.

The availability of a Focal Plane Polarimeter (FPP) to measure recoil proton polarization as standard experimental tool in Hall A at Thomas Jefferson National Accelerator Facility motivated the E91-011 proposal to study the N$\rightarrow\Delta(1232)$ transition through the measurement of polarization observables. Merits of this technique can be found in ref. [9, 10] and can be summarized as giving access to a simultaneous measurement of many

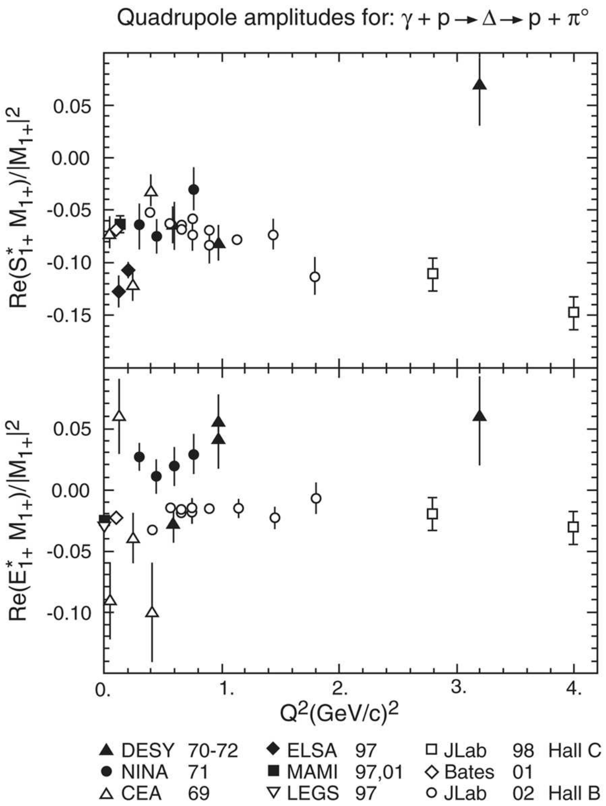

Figure 1. Q^2 dependence of the Coulomb (S_{1+}) and electric (E_{1+}) quadrupole/magnetic dipole ratios. Only statistical errors are shown. Data points are from DESY [1, 2, 3], NINA [4], CEA [5], ELSA [11], MAMI [12, 16], LEGS [13], Jlab [14, 15], Bates [18].

Response Functions (see next section) and to the determination of both real and imaginary parts of interference amplitudes.

This last feature is of particular importance when resonant and non-resonant parts contribute to the yield at the peak of a resonance. Scattering amplitudes can be decomposed in multipole amplitudes and all observables can be written as a sum of bilinear products of multipoles amplitudes. At the resonance peak, resonant amplitudes are purely imaginary and background amplitudes are essentially real, then the interference term with the M_{1+} amplitude has only a real part for a small resonant amplitude and only an imaginary part for a non resonant amplitude. These constraints allow, in principle, resonant and non-resonant contributions to be characterized.

The technique has already been used at lower momentum transfer in two experiments [16, 17] that have carried out the measurement only in parallel kinematics, when the proton is detected along the direction of momentum transfer. The E91-011 experiment has covered a large fraction of the kinematical phase space and the technical possibility of the extraction of the Response Functions (RFs) through recoil polarization measurements can be fully tested.

2. Extraction of Response Functions from Polarization Observables

Studying exclusive or semi-exclusive (semi-inclusive) reactions induced by polarized charged leptons with the detection, in coincidence with the scattered lepton, of one other final state particle, when the polarization of the target or of the detected outgoing particle is determined, allows the extraction of a wealth of information on the characteristic of the transition between the initial and the final states of the system under study. This will be discussed specifically for the reaction studied and afterwards some considerations will be added for a more general case.

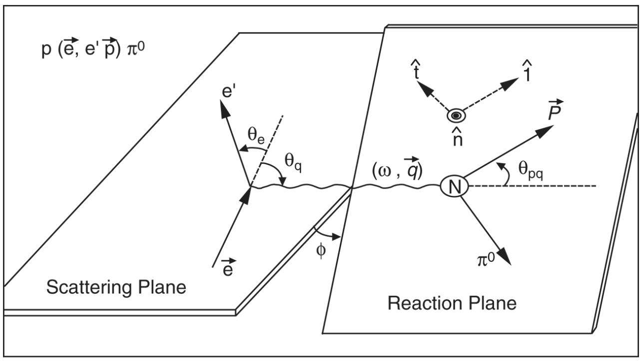

Figure 2. Kinematical variables relevant for the reaction under study. Capability to detect out-of-plane reactions is determined by the ϕ (azimuthal angle) acceptance of the detection apparatus at different θ_{pq} values.

In figure 2 some kinematical notations relevant for the scattering process considered are shown.

The cross section for the $p(\vec{e}, e'\vec{p})\pi^0$ process follows the general expression for a reaction induced by a polarized electron off an unpolarized target and when the polarization of the outgoing proton is measured that is given by [19, 20]:

$$\frac{d^5\sigma}{de' d\Omega_e d\Omega_p} \approx \sigma_0[1 + \mathbf{P} \cdot \mathbf{S} + \mathrm{h}(\mathrm{A_e} + \mathbf{P}' \cdot \mathbf{S})] \qquad (1)$$

where σ_0 is the five-fold unpolarized differential cross section, $\mathbf{S}$, $\mathbf{P}$ and $\mathbf{P}'$ are the spin, the induced and transferred polarizations of the outgoing proton, respectively, h is the beam helicity and A_e is the beam analysing power. Equation (1) refers to an exclusive process but a similar relation, with the cross sections now six-fold differential (adding the proton momentum differential), also holds for semi-exclusive (semi-inclusive) processes.

In figure 3 the relations between the measurable quantities of equation (1) and the Response Functions are shown.

18 Response Functions

$$\sigma_O = \nu_L \boxed{R_L} + \nu_T \boxed{R_T} + \nu_{LT} \boxed{R_{LT}} \cos\phi + \nu_{TT} \boxed{R_{TT}} \cos 2\phi$$

$$P_n \sigma_O = \nu_L \boxed{R_L^n} + \nu_T \boxed{R_T^n} + \nu_{LT} \boxed{R_{LT}^n} \cos\phi + \nu_{TT} \boxed{R_{TT}^n} \cos 2\phi$$

$$P_{l,t} \sigma_O = \nu_{LT} \boxed{R_{LT}^{l,t}} \sin\phi + \nu_{TT} \boxed{R_{TT}^{l,t}} \sin 2\phi$$

$$A_e \sigma_O = \nu'_{LT} \boxed{R'_{LT}} \sin\phi$$

$$P'_n \sigma_O = \nu'_{LT} \boxed{R'^{n}_{LT}} \sin\phi$$

$$P'_{l,t} \sigma_O = \nu'_{LT} \boxed{R'^{l,t}_{LT}} \cos\phi + \nu'_{TT} \boxed{R'^{l,t}_{TT}}$$

How to separate:

handle	Real type	Imaginary type
Left/Right	$\boxed{R_{LT}}, \boxed{R'^{l,t}_{LT}}, \boxed{R'^{l,t}_{TT}}$	$\boxed{R^n_{LT}}$
Out of plane	$\boxed{R_{TT}}, \boxed{R'^{n}_{LT}}, \boxed{R^n_{TT}}$	$\boxed{R'_{LT}}, \boxed{R^{l,t}_{LT}}, \boxed{R^{l,t}_{TT}}$
Rosenbluth	$\boxed{R_L}, \boxed{R_T}$	$\boxed{R^n_L}, \boxed{R^n_T}$

Figure 3. Relations between measured quantities and Response Functions. Methodology to extract individual Response Functions.

The ν are factors dependent on the electron kinematical variables, ϕ is the angle between scattering and reaction planes, the subscripts L,T,LT and TT refer to the longitudinal, transverse components of the hadronic tensor and interference between longitudinal and in plane transverse components and interference between in plane and orthogonal transverse components of the hadronic tensor respectively, all referring to the scattering plane and direction of the three-momentum transfer, the indexes l,n,t refer to the proton polarization components according to the reference system of figure 2, while unprimed and primed refer to beam helicity independent and dependent terms, respectively.

RFs are dependent on four scalar arguments that are usually chosen as the quadrimomentum transfer Q^2, the center-of-mass energy W, recoil proton momentum p and emission angle of the recoil proton with respect to the three momentum transfer θ_{pq}.

In figure 3 the methodology to single out the different RFs is also indicated. For fixed values of the arguments of the RFs, terms containing $\cos\phi$ allow extraction with a substraction from measurements carried out in plane at left/right of three momentum transfer ($\phi = 0^o$ and 180^o), terms containing $\sin\phi$, $\sin 2\phi$ or $\cos 2\phi$ need instead combination of out-of-plane ($\phi \neq 0^o$ or 180^o) measurements. All the mentioned measurements are carried out at the same kinematical values of incident and scattering electron variables, while for longitudinal and transverse RFs a Rosenbluth separation is required with different values of ν_L and ν_T obtained changing electron kinematics. Unprimed and primed RFs are separated combining measurements with opposite beam helicity.

RFs are real or imaginary parts of bilinear products of amplitudes and from the inset table in figure 3 is evident how polarization measurements are essential to determine both parts.

For a process, involving n particles with intrinsic spin j_i, in which the parity is conserved, the number of independent scattering amplitudes is given by $N = \prod_{i=1}^{n}(2j_i + 1)/2$, resulting in 2N-1 real parameters with one overall phase undeterminable. In the limit of the one photon (j=1) exchange approximation, our reaction is then described by 6 linearly independent complex scattering amplitudes and 11 real parameters which can be determined with opportunely chosen measurements [19, 21] which give the maximum obtainable knowledge of the reaction.

Naturally the determination of as many as possible RFs gives constraints on the derived scattering amplitudes.

A similar strategy to extract RFs can be applied if, instead of measuring the polarization of the outgoing proton, the polarization of the target is defined and the asymmetries of the reaction are measured when the target spin is flipped in different directions. In this case, analogous to equation (1), the cross section is given by [22, 23]:

$$\frac{d^5\sigma}{de' d\Omega_e d\Omega_p} \approx \sigma_0[1 + \mathbf{A}\cdot\mathbf{S} + \mathrm{h}(\mathrm{A_e} + \mathbf{A}'\cdot\mathbf{S})] \tag{2}$$

where $\mathbf{S}$, $\mathbf{A}$ and $\mathbf{A}'$ are the vector polarization of the target, the target analysing power independent and dependent (spin correlation coefficient in the more usual jargon of polarization experiments) respectively, from the beam helicity. The components of these last two vectors are determined through asymmetries measurements of the target polarized in the direction of the axis of the reference system with unpolarized and polarized beam.

Relations analogous to those of figure 3 hold for helicity independent and dependent target analysing power components and the 18 RFs that are now referred as target polarization RFs. The two sets of RFs - target polarization and recoil polarization - are clearly related to each other.

It has been shown [21] that to have the complete determination of the 11 parameters mentioned above only one set of measurements is not enough without at least one experiment from the other polarization set, while experiments with both target and recoil polarization are not necessary for the complete determination of the process.

The number of RFs that is required in the description of a reaction induced by a charged lepton beam depends on the spin of the polarized target or of the detected particle whose polarization is measured, for instance for a spin 1 particle the total number of RFs becomes 33 [9] instead of the 18 for a spin 1/2 particle.

As mentioned, the number of linearly independent scattering amplitudes depends on the spins of all the particles in the initial and final states of the reaction. For deuteron electrodisintegration or for Virtual Compton Scattering off a proton this number is 18, which implies the measurements of 35 selected parameters [24].

The structure of the cross section according to equations (1,2) and its dependence on 18 RFs derives from very general invariance properties of the hadronic tensor [25, 26] such as hermiticity, current and parity conservation. Then, it holds for every reaction induced by a longitudinal polarized charged lepton beam diffusing off a polarized spin 1/2 target with the detection of one hadron in the final state in coincidence with the diffused lepton or when the diffusion is on an unpolarized target with arbitrary spin but the detected hadron is a 1/2 spin particle and its polarization is measured. Independently from the energy scale of the reaction, the general formulation is valid in the region of single levels nuclear excitation, giant dipole resonance, quasifree nucleon scattering, resonances electroproduction and also for exclusive or semi-inclusive deep inelastic (SIDIS), an energy regime more in the focus of this workshop.

In SIDIS regime models describe the reaction at the parton level. The simplest diagram representing the squared amplitude at leading order is shown in figure 4a. The hadronic tensor contains two soft parts represented by the blobs in the figure, these parts contain the relevant information on the hadron structure at the parton level and on the quark-hadron dynamic. Φ contains information on how the momentum and spin of the quarks is distributed in the target hadron (distribution functions), Δ is the correlator giving the production probabilities of the final hadron from the quark that has been scattered in the hard process with the virtual photon (fragmentation functions).

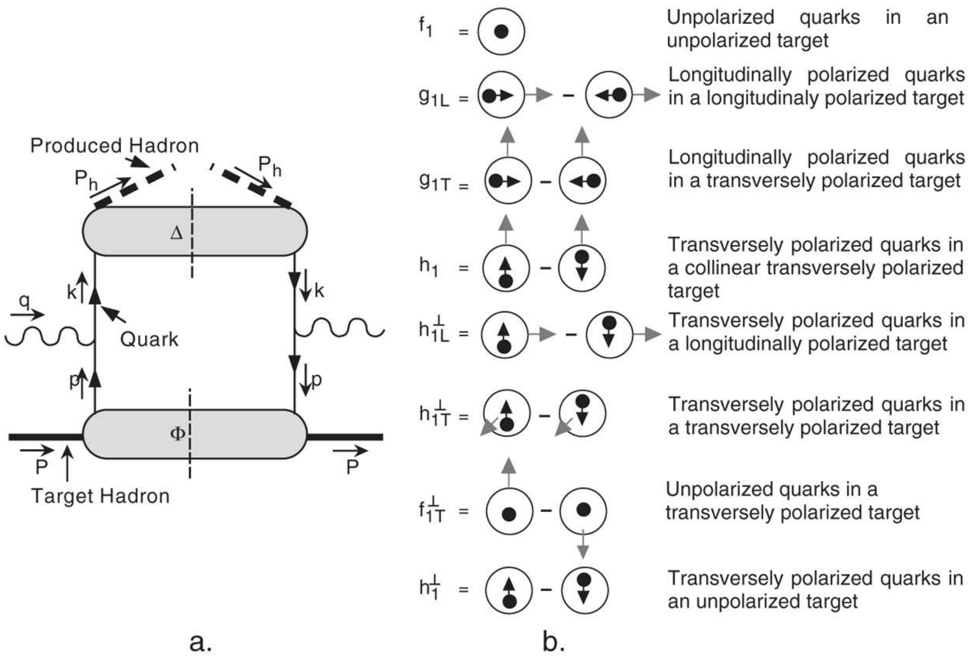

Figure 4. Semi-inclusive scattering process (a.) and leading order distribution functions (b.). Adapted from [27].

In figure 4b the leading order (twist two) distribution functions are shown. They appear as combinations of measurements with unpolarized and polarized targets with different polarization directions and they are interpreted as parton momentum or spin densities in unpolarized or polarized targets [27]. Other distribution functions appear at higher subleading orders but are not interpretable as densities or differences of densities. A description of the process up to twist three is available [28]. A complete strategy to single out the functions of interest has not been found yet.

SIDIS induced by polarized leptons off polarized protons can be described by a cross section of the type of equation (2), while the study of semi-inclusive Λ production from an unpolarized target with determination of its polarization through the self analysing power of its weak decay is described by equation (1). As said, in both cases a well established strategy exists to extract single RFs. Then, particularly important is a more transparent deduction, in the framework of SIDIS models, of the Response Functions in terms of distribution and fragmentation functions in order to evaluate if the methodology of extraction adopted can be of help also to single out the functions of interest in SIDIS regime, sharing a common practise and language with other related fields of lepton scattering.

3. E91-011 Measurements

The experiment has been carried out in Hall A at JLab [29], utilizing its two high resolution spectrometers. The strained GaAs source provided an electron beam with a longitudinal polarization that remained within 67 to 79% for all the time of data taking (35 days) at an average current of 45 μA, with the beam helicity flipping pseudorandomly at 30 Hz. The polarization was monitored continously by a Compton [30] and occasionally by a Møller polarimeter. The two measurements were in agreement within a few percent. A liquid H_2 target 15 cm long was used.

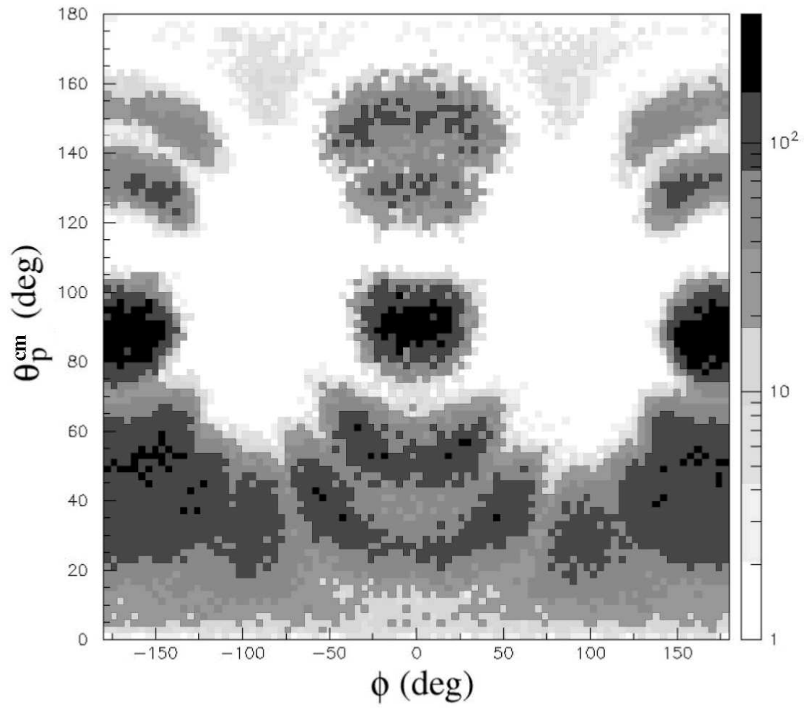

Figure 5. Angular coverage for the measurements. Contours of normalized yield are shown for (θ_p^{cm}, ϕ), combining acceptances of the various kinematical settings.

The electron kinematics has been kept fixed for all the kinematical sets of data production : incident and scattered electron energy = 4.535 and 3.066 GeV respectively, and electron scattering angle = 14.09^0, defining a $Q^2 = 1.0\ (GeV/c)^2$. Proton momenta and angles were chosen to have an invariant mass of the hadronic final system of W = 1.232 GeV and to cover in an adequate way the center-of-mass (COM) angular distribution.

In figure 5 the angular phase space coverage is shown. For all θ_p^{cm} settings, in plane measurements, centered at $\phi = 0^o$ and 180^o, were carried out to allow the extraction of 6 RFs with the "left/right" handle. The Lorentz boost limits the window of laboratory angle of the emitted particles and this results in a considerable ϕ acceptance for the settings with small values of θ_p^{cm}, allowing the extraction of other 8 RFs with the "out-of-plane" handle. For the other 4 RFs, a separated combination of longitudinal and transverse RFs is extracted for unpolarized and for n component induced polarization RFs. In addition, the measurement in parallel kinematics (θ_p^{cm} $= 0^o$) will allow the determination of R_L/R_T at that angle [31].

The Hall A High Resolution Spectrometer (HRS) pair was used for the detection of the electrons and protons. The electron arm included a two-plane scintillator array, providing triggering and time-of-flight information for coincident particle identification, as well as an atmospheric CO_2 threshold Čerenkov detector and a segmented lead glass calorimeter for π^-/e discrimination. In order to track trajectories, two vertical drift chambers each with a pair of wire planes were used. The proton arm included the same system of scintillators and tracking detector and in addition contained a focal plane polarimeter (FPP) [32] consisting of an adjustable thickness graphite analyzer sandwiched by straw tube drift chambers that allowed the measurement of polar and azimuthal angles after scattering in the analyzer.

The determination of the two components of the proton polarization at the FPP, transverse to the momentum, is accomplished through Fourier analysis of the angular distribution, using the known analyzing power of carbon for the energies of interest. Due to the precession of the proton spin in the different magnetic elements of the HRS, the polarization components at the target are different from the values measured at the FPP. They are related through a 3x3 spin transport matrix that depends on the proton trajectory and then is unique for each event. A maximum likelihood method [33] was used to obtain the polarization at the target.

To check the polarimetry analysis, several elastic $p(\vec{e}, e'\vec{p})$ measurements were carried out, with proton momenta spanning the range used in the settings of the experiment. In this way it has been possible to check/calibrate the instrumental asymmetries in the FPP, as well as cross check extracted polarizations with measurements already available.

All the components of the induced and transferred polarization at the target have been determined.

In figure 6, as an example, the azimuthal angular distributions of the n component of the induced polarization at the target for several intervals

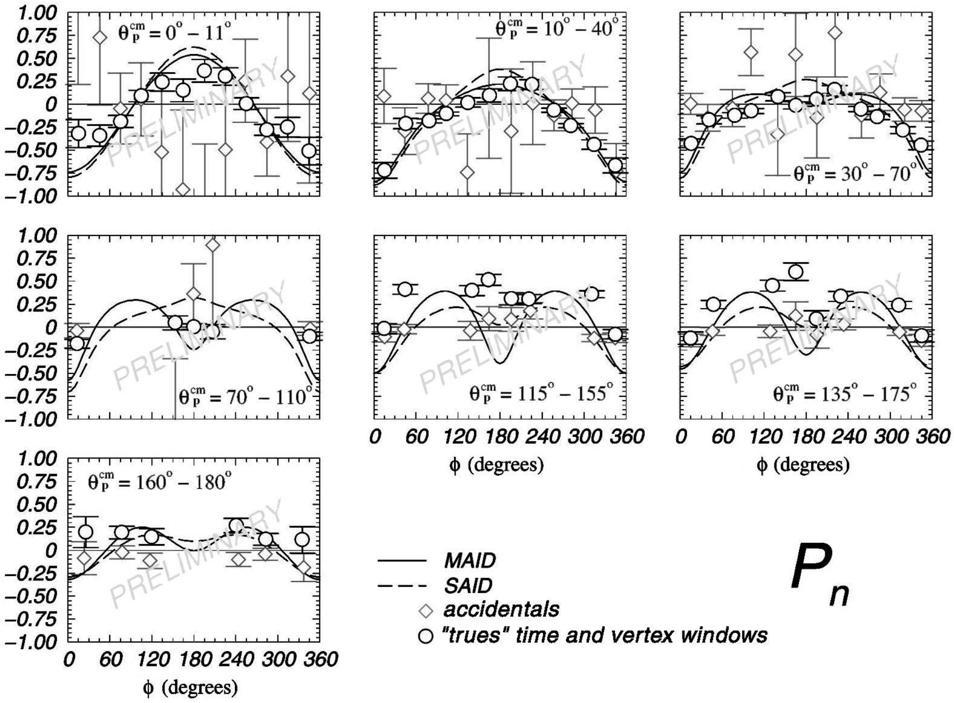

Figure 6. Azimuthal angular distributions of the induced polarization n component at target. Results are compared with SAID [34] and MAID [35] parametrizations.

of the COM angle are shown. Experimental points refer to the measured polarization for accidentals and the "trues", defined in the appropriate coincidence time and reconstructed target position windows, while curves are the results of computations using scattering amplitudes with parametrizations derived from a phase shift analysis of the world's data (SAID) [34] or from the Mainz unitary isobar model (MAID) [35].

To measure cross sections one must rely on a good knowledge of the phase space acceptance of the experimental apparatus. For all the experiment, selection of events was made applying cuts on the correlations between the reconstructed origin in the target and coincidence time, between the ADC level of the pulse from the scintillators of the hadron arm and the β of the particle and between missing mass and missing momentum. The results of a simulation, using the Hall A Monte Carlo simulator MCEEP with MAID as an event generator, of the spectrometers acceptances for all variables showed remarkable agreement with the shape of the measured distributions.

Azimuthal angular distributions of the unpolarized reduced cross section (σ_0 divided by the flux of the vitual photons) for some values of the pion

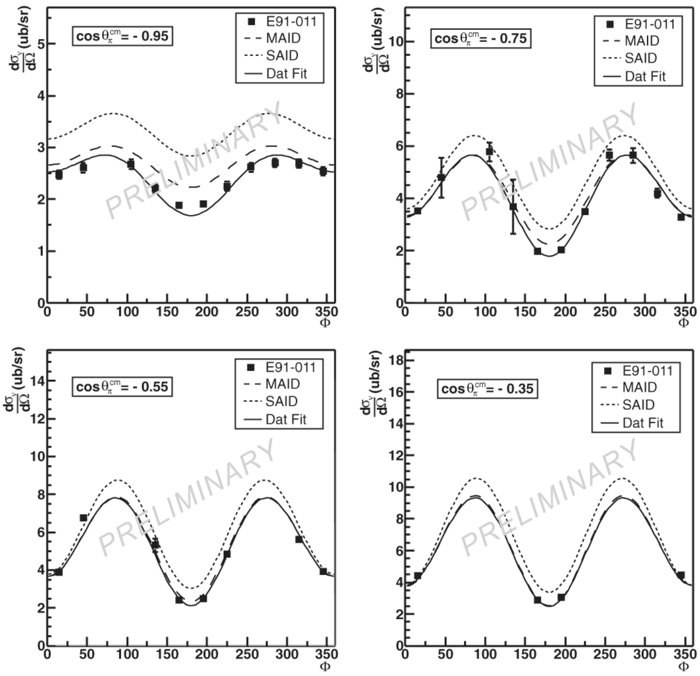

Figure 7. Azimuthal angular distributions of the unpolarized reduced cross section.

COM angle are shown in figure 7. The precision of the data points seems to be able to discriminate between models.

From the measured polarization components and unpolarized cross section it is possible to extract the Response Functions. This is again made using a maximum-likelihood method of the type used before but with the RFs having replaced the polarization components, according to the relations of figure 3, in the function to be minimized.

In figure 8 the extracted helicity-independent polarized RFs are shown. Data are compared with the results of SAID and MAID parametrizations and indicate that the data accuracy is good enough to discriminate between the two models that differ significantly due to the different weight of non resonant components of the amplitude. In the figure it is also shown that MCEEP simulation, that takes properly into account the detector acceptances, does not differ from the results obtained with the same parametrization (MAID) using kinematical values at the center of the acceptances, indicating that the eventual difference between data and a theoretical curve is not due to acceptance problems. In figure 8 , to extract RFs from the polarization data, the computed values (MCEEP with MAID) of the unpolarized cross section were used; work is in progress to use instead the

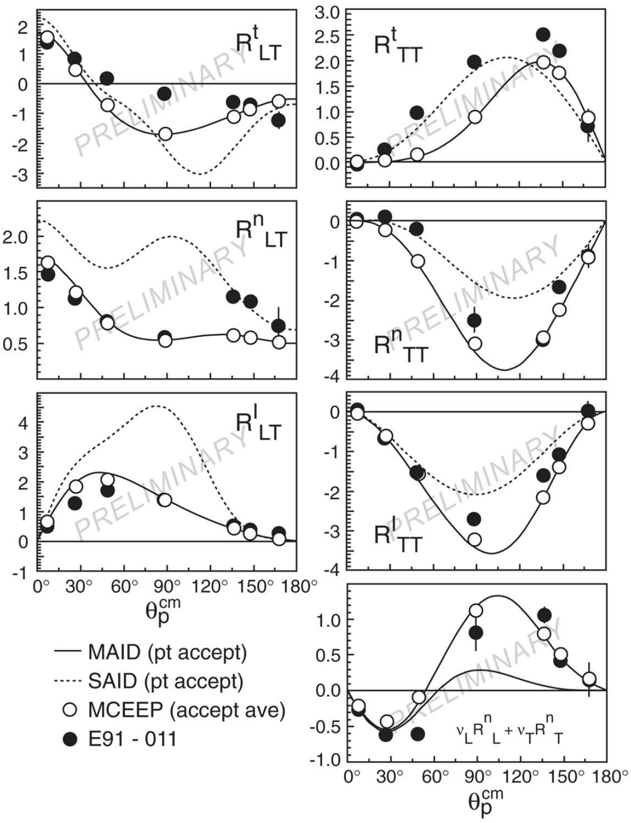

Figure 8. Helicity-independent polarization Response Functions. Results are compared with SAID [34] and MAID [35] parametrizations.

experimental measured values.

Work is also in progress to extract the unpolarized RFs. With all the RFs extracted, the multipole decomposition will be worked out with the aim to precisely quantify all the contributions to the N→Δ(1232) transition.

4. Conclusions and outlook

For the first time the simultaneous separation of many RFs with recoil polarization technique has been applied for measurements covering a large fraction of the phase space, for a single Q^2, W setting.

The technique has been proven valid and 14 RFs have been individually extracted within the same set of measurements with the additional information coming from two combinations of the other 4.

Multipole decomposition, the most model independent analysis that can be made, is still to be done. Its result should give the physical information about the size of the small resonant and non resonant contributions. This is the physics aim of the experiment and will define the sensitivity of the technique. From this result one will infer the suitability to perform measurements at other Q^2, W settings or/and for other reactions.

The technique is applicable to leptoproduction experiments in higher energy regimes provided that models, supposed to describe hadronic systems in that regimes, offer the opportunity to test their predictions in terms of RFs.

This work was supported by DOE contract DE-AC05-84ER40150 under which the Southeastern Universities Research Association (SURA) operates the Thomas Jefferson National Acceleration Facility and in part by contract DE-FC02-94ER40818.

References

1. Albrecht, W. *et al.* (1970) *Nucl. Phys.* **B25**, 1
2. Albrecht, W. *et al.* (1971) *Nucl. Phys.***B27**, 615
3. Alder, J. C. *et al.* (1972) *Nucl. Phys.***B46**, 573
4. Siddle, R. *et al.* (1971) *Nucl. Phys.* **B35**, 93
5. Mistretta, C. *et al.* (1969) *Phys. Rev.* **184**, 1487
6. Isgur, N., Karl, G. and Koniuk, R. (1982) *Phys. Rev.* **D25**, 2394
7. Capstick, S. (1992) *Phys. Rev.* **D46**, 2864
8. Silva, A. *et al.* (2000) *Nucl. Phys.* **A675**, 637
9. Raskin, A. D. and Donnelly, T. W. (1989) *Ann. Phys.* **191**, 78
10. Lourie, R. W. (1992) *Phys. Rev.* **C45**, 540
11. Kalleicher,F. et al. (1997) *Z. Phys.* **A359**, 201
12. Beck, R. *et al.* (1997) *Phys. Rev. Lett.* **78**, 606
13. Blanpied, G. *et al.* (1997) *Phys. Rev. Lett.* **79**, 4337
14. Frolov, V. V. *et al.* (1999) *Phys. Rev. Lett.* **82**, 45
15. Joo, K. *et al.* (2002) *Phys. Rev. Lett.* **88**, 122001
16. Pospischil, Th. *et al.* (2001) *Phys. Rev. Lett.* **, 86**, 2959
17. Warren, G. A. *et al.* (1998) *Phys. Rev.* **C58**, 3722
18. Mertz, C. *et al.* (2001) *Phys. Rev. Lett.* **86**, 2963
19. Giusti, C. and Pacati, F. D. (1989) *Nuc. Phys.* **A504**, 685
20. Kelly, J. J. (1996) *Adv. Nuc. Phys.* **23**, 75
21. Dmitrasinovic, V.*et al.* (1987) Research Program at CEBAF (III), 547
22. Laget, J. M. (1991) *Phys. Lett.* **B273**, 367
23. Boffi, S., Giusti, C. and Pacati, F. D. (1993) *Phys. Rep.* **226**, 1
24. Dmitrasinovic, V. and Gross, F. (1989) *Phys. Rev.* **C40**, 2479
25. Gourdin, M. (1972) *Nucl. Phys.* **B49**, 501
26. Picklesimer, A. and Van Orden, J. W. (1987) *Phys. Rev.* **C35**, 266
27. Mulders, P. J. (2002) *Czech. Journ. Phys.* **52 Suppl. A**, A1
28. Mulders, P. J. and Tangerman, R. D. (1996) *Nucl. Phys.* **B461**, 197
29. Anderson, B. D. *et al.* submitted to *Nucl. Instrum. Meth. in Phys. Res.*
30. Baylac, M. *et al.* (2002) *Phys. Lett.* **B539**, 8
31. Kelly, J. J. (1999) *Phys. Rev.* **C60**, 054611
32. Bimbot, L. *et al.* submitted to *Nucl. Instrum. Meth. in Phys. Res.*
33. Wijesooriya, K. *et al.* (2002) *Phys. Rev.* **C66**, 034614
34. Arndt, R. A., Strokovsky, I. I. and Workman, R. L. (1996) *Phys. Rev.* **C53**, 430
35. Drechsel, D. *et al.* (1999) *Nucl. Phys.* **A645**, 145
36. Ulmer, P. www.physics.odu.edu/ulmer/mceep/mceep.html